Fabrication and Characterization of Nanostructured Functionally Graded Ni-P Electroless Coating

Sayede Razieh Anvari[1*], Sayed Mahmoud Monirvaghefi[2], Mohammad Hossien Enayati[2]

[1] Young Researchers and Elite Club, Najafabad Branch, Islamic Azad University, Najafabad, Iran;
[2] Department of Materials Engineering, Isfahan University of Technology, Isfahan, Iran

ARTICLE INFO

Article history:

Received 22 January 2016
Accepted 1 March 2016
Available online 1 April 2016

Keywords:

Electroless
Nickel-phosphorus
Stainless steel
Functionally graded coating
Nano-indentation.

ABSTRACT

Abstract

In this research, novel functionally graded Ni-P coating was deposited via electroless process. The content of phosphorus was controlled to change gradually through the thickness of the coating. During the plating, bath temperature and pH changed at specified intervals to obtain a functionally graded structure. To compare the properties of functionally graded coating with the Ni-P single-layer coatings, three types of coatings with different phosphorus contents were also deposited. Microstructure and phase composition of the coatings were studied by scanning electron microscopy (SEM), transmission electron microscopy (TEM) and X-ray diffractometry (XRD). The mechanical properties and tribological behavior of the coatings were also investigated. Low phosphorus and medium phosphorus single-layer coatings had fully crystalline and amorphous-crystalline structures, respectively. While high phosphorus coating appeared to have a fully amorphous structure. TEM images showed that low phosphorus coating had a nano-crystalline structure. Results of nano-indentation test showed gradual changes in hardness profile in the cross-section of functionally graded coating due to the gradual changes of the phosphorus content in the thickness of this coating. According to the wear test data, medium phosphorus coating had minimum wear resistance. Functionally graded coatings had better wear resistance than single-layer coatings.

1. Introduction

Nickel-phosphorus electroless plating is widely used to improve materials properties. This surface process provides coatings with uniform thickness, corrosion resistance, high hardness and wear resistance [1-5]. The properties of these coatings depend on their structural characteristics. One of the most important factor affecting the properties and structure of these coatings is phosphorus content [6-8]. So that with decreasing phosphorus content the structure of coatings would be changed from amorphous to crystalline [6,7,9,10]. As a result, wear resistance and hardness of coatings would be changed by increasing phosphorus content. Recently, graded coatings have received much attention for better mechanical and tribological properties. Furthermore, for increasing resistance of coatings

* Corresponding Author:
E-mail address: sr.anvari@ma.iut.ac.ir

to functional failure, functionally graded coatings are being studied in coating design and developed by scientists [11-16]. As it is mentioned, one of the appropriate methods for improving surface properties of material is electroless plating. Although, some researchers deposited graded coatings with electroless plating, but for this purpose, they had used sequential immersion in different baths (Ni-P or Ni-P and Ni-B) [17-19]. In these methods, the coated samples after each step must be transferred from one bath to another one, which may cause poor adhesion between separate layers of coatings. Due to the mentioned problem and also due to the lack of published results in literature, in this study functionally graded coating (FGC) was fabricated by using one electroless bath while pH and temperature of bath were changed at certain intervals during plating. Chemical composition, structure, wear resistance and hardness of this coating were also characterized and compared with single layer coatings.

2. Experimental procedures

In this study, electroless coatings were deposited on martensitic stainless steel substrates. To prepare the substrates for plating, the pretreatment processes were applied according to Table 1.

Table 1. The details of pretreatment processes.

Process sequence
1- grinding the samples over SiC paper from 80 to 800 grades
2- washing the samples with distilled water
3- electrocleaning in 1 normal NaOH solution at 5 volts for 2 minutes
4- washing the samples with distilled water
5-immersion in 30% HCl solution for 1 minute
6- immersion in a nickel electric bath containing $NaCl_2.6H_2O$ and HCl in $10A/dm^2$ current for 1 minute

Finally after washing samples with distilled water, they were entered the electroless plating bath. The commercial nickel phosphorous electroless solution (Schloter SLOTONIP70A) including nickel sulfate, NaH_2PO_4 as reducer and suitable values of additive and stabilizer were used. A 1 liter double wall beaker connected to a thermo stated circulating water was used as a container. Coating bath was stirred by a PTFE coated magnet. According to the conditions given in Table 2, there single-layer electroless coatings were fabricated. Then the effects of phosphorus content on structure, mechanical and tribological properties of single-layer coatings was studied. In order to deposit functionally graded coating (FGC), temperature and pH of the bath were changed at certain intervals during the plating as shown in Fig 1. The mechanical properties of coatings were investigated in the cross-section using a nano-indenter NHTX S/N:01-03119. X-ray diffraction, (XRD, Cu Kα) analysis was used to identify the phases in the coatings. The structure of coatings were studied by transmission electron microscopy (TEM, CM120FEG) and scanning electron microscopy (SEM, Philips-XL30). Energy-dispersive X-ray spectroscopy (EDS) was used to analyze phosphorous contents of coatings. For single-layer coatings crystallite size was calculated from XRD pattern by using Williamson-Hall method [20]. The wear behavior of coatings was evaluated by using a pin-on-disc wear tester under normal load of 35 N. Wear tests were performed under non-lubricated conditions, at the ambient temperature. The wear tests were done against AISI 52100 steel pin with 5 mm in diameter. Surftest SJ-210 (Mitotoyo) profilometer was used to detect the depth profiles of the wear tracks.

Table 2. Temperature and pH conditions of electroless bath for single-layer coatings.

Coatings	pH	Temperature(∘C)
low P	7±0.1	75±1
medium P	5.5±0.1	85±1
high P	4±0.1	91±1

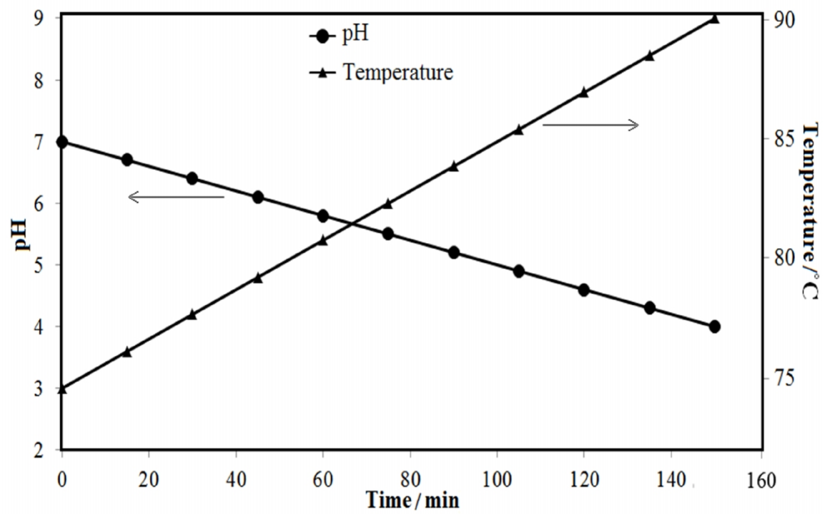

Fig 1. Temperature and pH conditions of electroless bath for L-H FGC.

3. Result and discussion

3.1. Structure of coatings

Fig. 2 shows the cross-section of L-H FGC, which is made of gradual change in phosphorus content from 12.3wt.% at the top to 3wt.% near the substrate (Fig. 3). According to Fig. 2 the coating has uniform thickness and appropriate adhesion to the substrate. Fig.4 shows cross-section of a graded Ni-P coating reported by Narayanan et al., which is deposited by using three different bathes [17]. As it is clear in Fig. 4, non-uniform interfaces are observable between different layers [17].

Fig. 5 shows the results of EDS analysis for single-layer coatings. According to this figure, three types of low phosphorous coatings (low P) with 3.0wt.%P, medium phosphorous (medium P) with 6.4wt.%P and high phosphorus (high P) with 12.2wt.%P were successfully fabricated by using same basic bath and changing the conditions of deposition. The thickness of deposited Ni-P coatings is 50 ± 5μm. Fig. 6 shows X-ray diffraction patterns for three kinds of single-layer coatings, this figure also confirms formation of three different coatings by the same basic bath in different temperature and pH conditions.

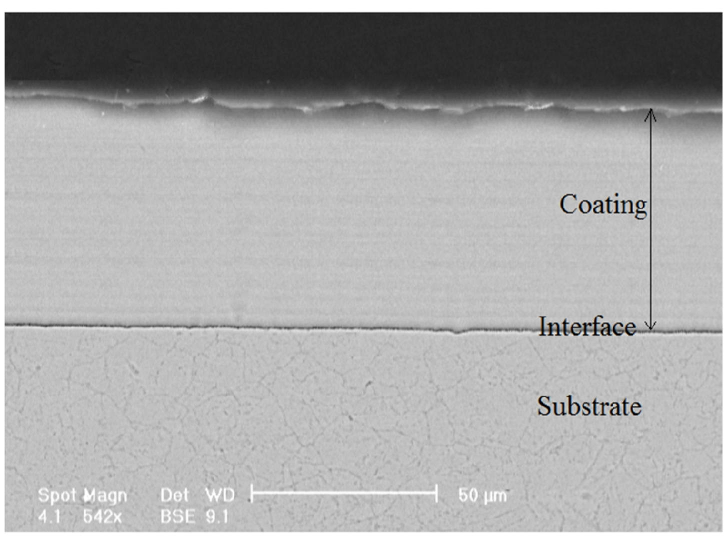

Fig 2. Cross-sectional micrograph of L-H functionally graded Ni-P coating.

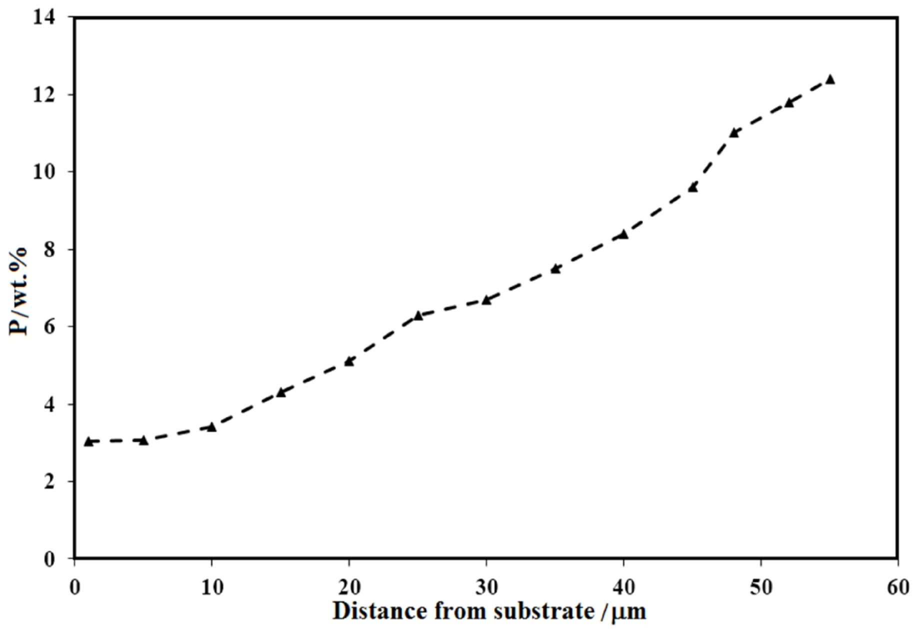

Fig 3. Amount of phosphorus content through thickness of L-H FGC.

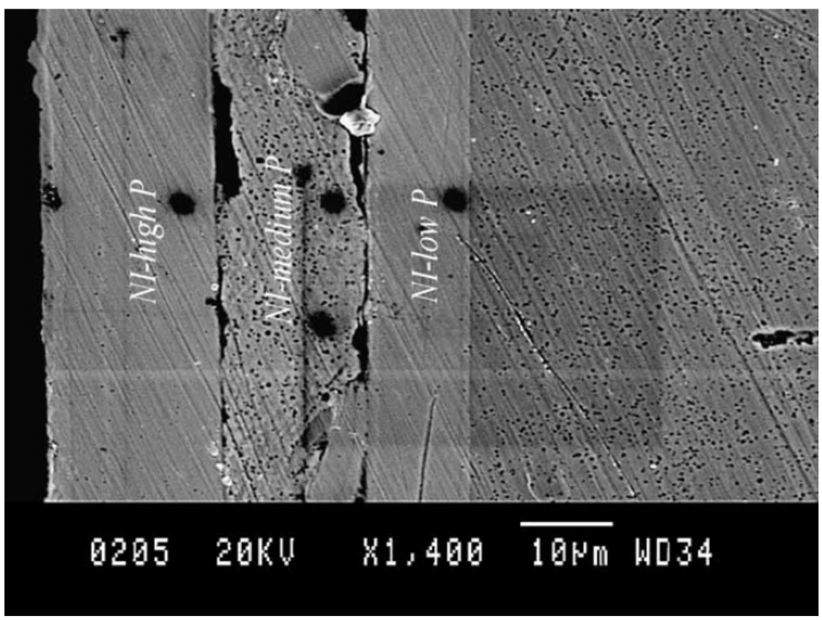

Fig 4. Cross sectional micrograph of graded electroless Ni-P (LMH) coating [17].

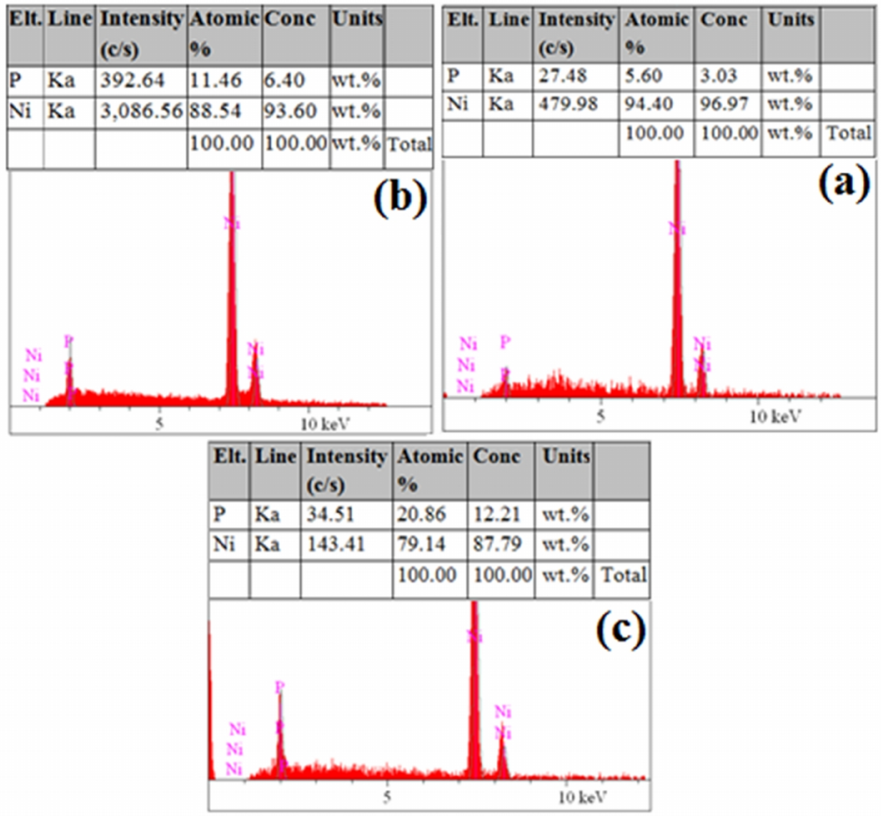

(b)

Elt.	Line	Intensity (c/s)	Atomic %	Conc	Units	
P	Ka	392.64	11.46	6.40	wt.%	
Ni	Ka	3,086.56	88.54	93.60	wt.%	
			100.00	100.00	wt.%	Total

(a)

Elt.	Line	Intensity (c/s)	Atomic %	Conc	Units	
P	Ka	27.48	5.60	3.03	wt.%	
Ni	Ka	479.98	94.40	96.97	wt.%	
			100.00	100.00	wt.%	Total

(c)

Elt.	Line	Intensity (c/s)	Atomic %	Conc	Units	
P	Ka	34.51	20.86	12.21	wt.%	
Ni	Ka	143.41	79.14	87.79	wt.%	
			100.00	100.00	wt.%	Total

Fig 5. EDS analysis for (a) low P, (b) medium P and (c) high P single-layer coatings.

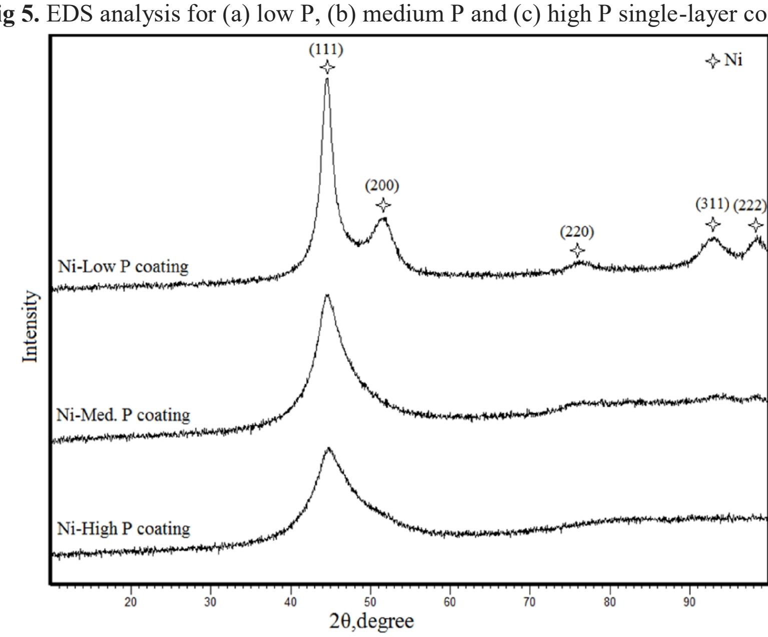

Fig 6. X-ray diffraction patterns for as plated low P, medium P and high P coatings.

As seen in Fig. 7 low P (3.0wt.%P) coating has a crystalline structure. Crystallite size of this coating was estimated to be 9±2 nm by using Williamson-Hall method. For high P coating the broad peak at about 45˚ suggests an amorphous structure. Furthermore, medium P coating contains a mixture of amorphous and crystalline structures. TEM image of low P coating (Fig. 7) confirms nano sized crystals of nickel. Also, for high P coating TEM image confirms amorphous structure (Fig. 8).

3.2. Mechanical properties

Nano-indentation test was performed at the cross-section of coatings to obtain the values of hardness and elastic modulus. Fig. 9-a shows F-h curves for single-layer coatings. With increasing load, penetration depth of the indenter increases until it reaches its maximum. The hardness and elasticity modulus obtained from these graphs are presented in Fig. 9-b. Hardness data in Fig. 9 indicates that among the single-layer coatings, high P coating has the minimum hardness, and low P coating has the maximum. In fact, low P coating includes a single β-phase which is a crystalline solution of phosphorus in nickel and high P coating includes γ-phase which has amorphous structure[10]. Since β-phase with nano crystalline structure has more hardness than γ-phase, so the hardness of coatings would be decreased with increasing phosphorus content. Fig. 10 shows nano-indentation test results for L-H FGC. This figure indicates gradual hardness profile in cross-section L-H FGC, which is as a result of gradual changes in phosphorus content and so that changes in the microstructure of coating through the thickness. L-H FGC has decreasing hardness through the thickness from the substrate to surface of coating.

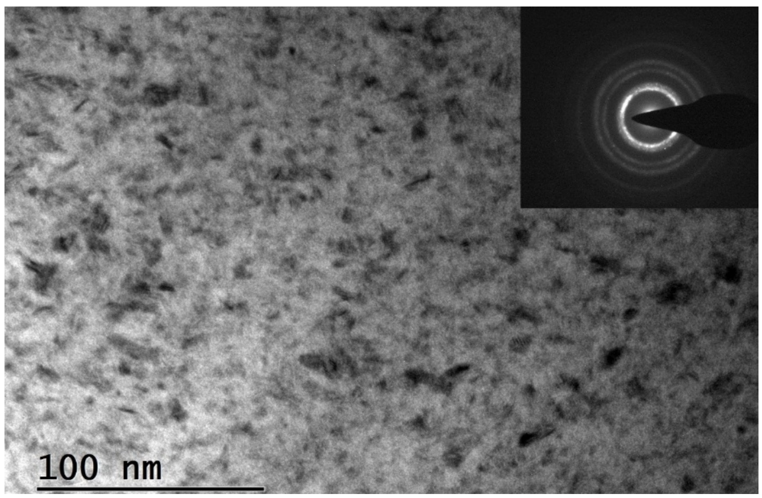

Fig 7. TEM image of low P coating.

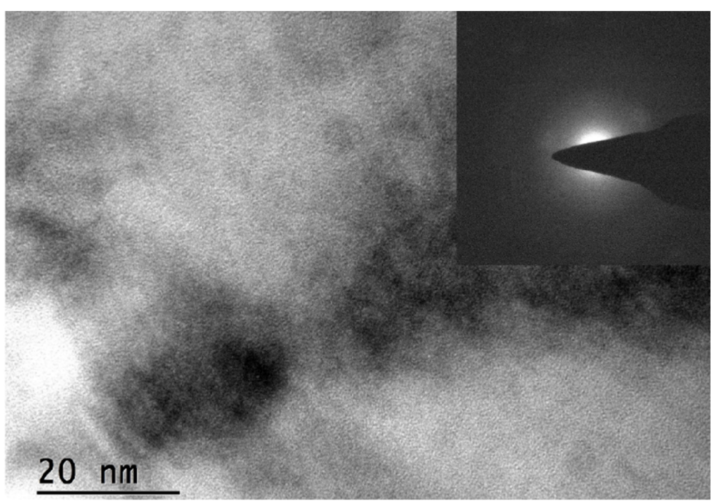

Fig 8. TEM image of high P coating.

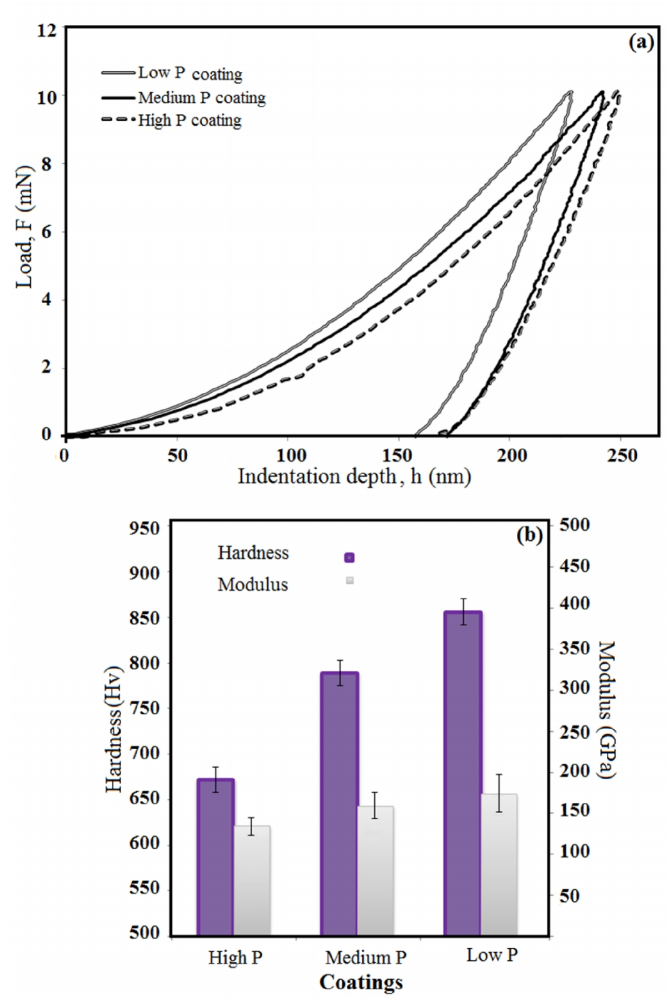

Fig 9. (a) Load–Indentation depth curves, (b) hardness and elasticity modulus for single-layer coatings.

3.3. Wear behavior

Wear behavior of coatings and effect of phosphorus content and its gradual changes through the thickness of FGC on wear resistance were studied. Fig. 11 shows the relationship between wear loss and sliding distance for coatings. Fig. 12 indicates depth and width of wear track for coatings. According to this figure, the maximum wear depth is about 38 µm, since the thickness of coatings are about 50 µm, it can be concluded that the wear test could not completely destroy the coatings, and steel pin didn't contact the substrate. From figures 11 and 12 it can be concluded that medium P coating has the minimum wear resistance, while its hardness is more than high P coating. Although hardness is considered as a primary mechanical property which determines wear resistance of material, but it is not the only determining factor for wear resistance [21]. There is strong evidence that suggests the elasticity modulus can also have a main effect on wear behavior. Some authors believed that H/E ratio is a suitable criterion for evaluating wear properties of materials. It is also significant that the ratio between H and E, which is so-called plasticity index, is a main measure for determining the limit of elastic behavior in surface contact, which is clearly valuable for prevention of wear. Especially, the elastic strain to failure, which is dependent on the ratio of hardness (H) and elastic modulus (E), has been indicated by a number of authors to be a more appropriate parameter than hardness for predicting wear resistance. Generally the more the H/E ratio, the better wear resistance [22,23]. Table 3 presents H/E ratios of single-layer coatings from results of nano-indentation test. According to results, for medium P has the lowest H/E ratio among the single-layer coatings. So it may be concluded that its poor wear resistance between coatings is related to its H/E ratio. As figures 11 and 12 indicate, FGC has more wear resistance than single-layer coatings. Wang et al. suggested that for FGC, cracks were effectively prevented due to the introduction of gradual changes in composition through the thickness of coatings, relatively fine cracks were propagated on the wear track of the graded coating thus inhibiting catastrophic failure under the heavy load [24].

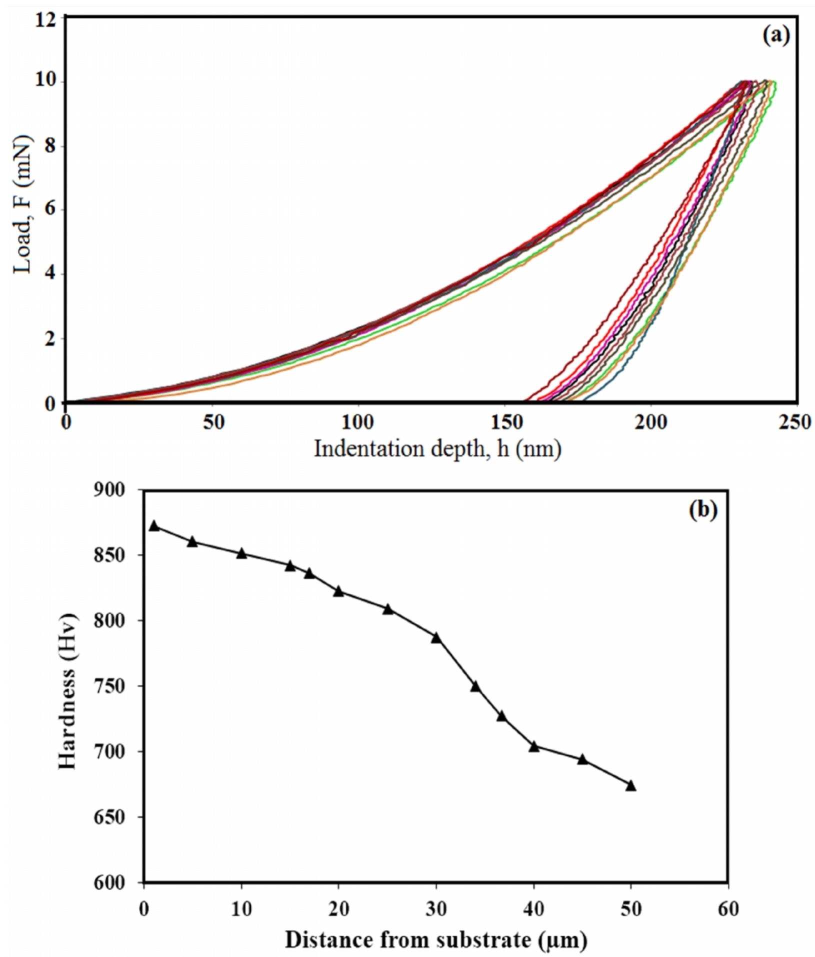

Fig 10. (a) Load–Indentation depth curves, (b) hardness and elasticity modulus for L-H FGC.

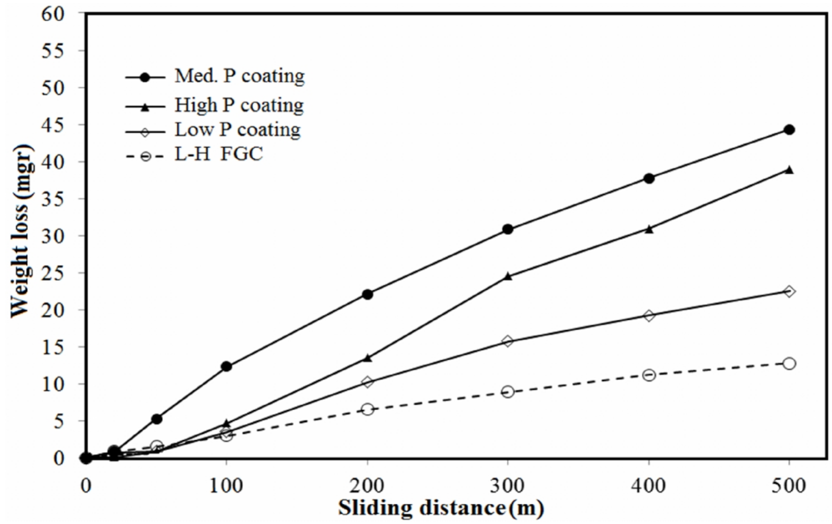

Fig 11. Weight loss of base metal and coatings as a function of sliding distance.

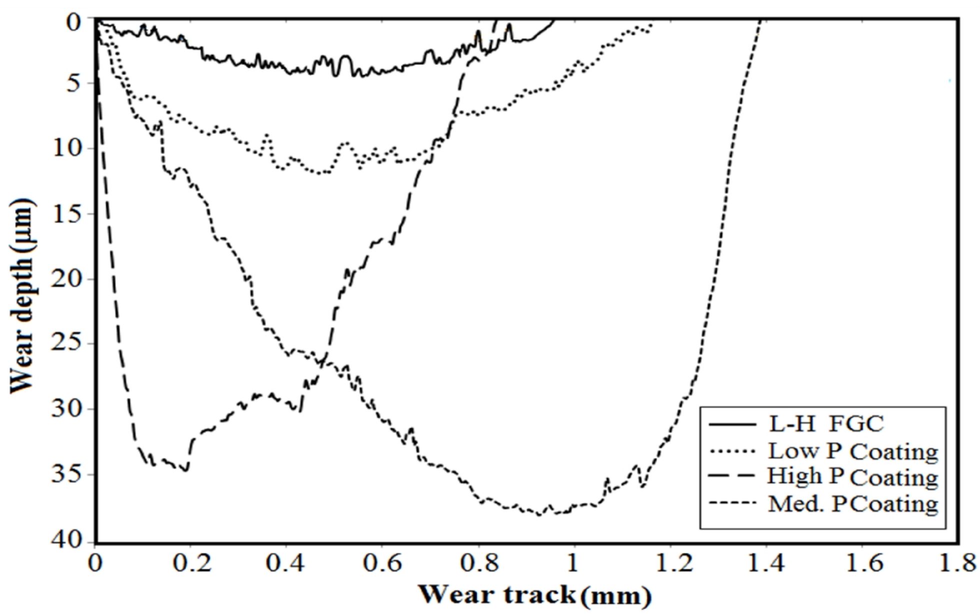

Fig 12. Weight loss of coatings as function of sliding distance.

Table 3. H/E ratios calculated from the nano-indentation tests on single layer coatings.

Coating	H/E /$\times 10^{-3}$
Low P	52.35
Medium P	48.71
High P	50.80

Conclusions

1- As deposited low P coating had nano sized structure, medium P coating contained a mixture of amorphous and crystalline structure and high P coating had amorphous structure.

2- Nano indentation test results showed hardness profile in cross section of functionally graded coating which indicated changes through the thickness.

3- Among the single-layer coatings, low phosphorus coating had the maximum hardness and H/E ratio due to the presence of hard nano-structure β phase, and also exhibited maximum wear resistance among all single-layer coatings.

4- Medium phosphorus coating had the minimum wear resistance, while its hardness was not minimum. The main reason may be that medium phosphorus coating had the minimum H/E ratio, and this ratio is a more appropriate parameter than hardness for predicting wear resistance.

5- Functionally graded coating sindicated much better wear resistance than single-layer coatings because the gradual changes in its composition and structure prevents from cracks propagation through the thickness.

References

[1] A. Zarebidaki and S. R. Allahkaram, "Porosity measurement of electroless Ni–P coatings reinforced by CNT or SiC particles," Surf. Eng., vol. 28, pp. 400–405, 2012.

[2] C. L. Ban, X. Shao, and L. P. Wang, "Ultrasonic irradiation assisted electroless Ni–P coating on magnesium alloy," Surf. Eng., vol. 30, pp. 880–885, 2014.

[3] M. H. Sadhir, M. Saranya, M. Aravind, A. Srinivasan, A. Siddharthan, and N. Rajendran, "Comparison of in situ and ex situ reduced graphene oxide reinforced electroless nickel phosphorus nanocomposite coating," Appl. Surf. Sci., vol. 320, pp. 171–176, 2014.

[4] S. Alirezaei, S. M. Monirvaghefi, A. Saatchi, and A. Motallebzadeh, "High temperature tribology of nanocrystalline Ni – P – Ag coating," Surf. Eng., vol. 29, no. 4, pp. 306–311, 2013.

[5] L. L. Wang, H. J. Chen, and Z. L. Chen, "Study on post-treatments for electroless Ni–P coating," Surf. Eng., vol. 27, pp. 57–60, 2011.

[6] S. H. Park and D. N. Lee, "A study on the microstructure and phase transformation of electroless nickel deposits," J. Mater. Sci., vol. 23, no. 5, pp. 1643–1654, 1988.

[7] A. W. Goldstein, W. Rostoker, and J. J. Rezek, "Electron microscope study of the nucleation and growth of electroless cobalt and nickel," J. Electrochem. Soc., vol. 119, pp. 1614–1619, 1972.

[8] E. Vafaei-Makhsoos, E. L. Thomas, and E. L. Toth, "Electron microscopy of crystalline and amorphous Ni-P electrodeposited films: in-situ crystallization of an amorphous solid," Metall. Trans. A, vol. 9, pp. 1449–1460, 1978.

[9] B. Jiang, L. Xiao, S. Hu, J. Peng, H. Zhang, and M. Wang, "Optimization and kinetics of electroless Ni–P–B plating of quartz optical fiber," Opt. Mater., vol. 31, no. 10, pp. 1532–1539, 2009.

[10] R. Taheri, "Evaluation of Electroless Nickel-Phosphorus (EN) Coatings," PhD Thesis, no. August 2002, 2003.

[11] R. K. Upadhyay and L. A. Kumaraswamidhas, "Surface modification by multilayered W/W2N coating," Surf. Eng., vol. 30, pp. 475–482, 2014.

[12] F. Gao, Q. Yang, R. Liu, and X. Huang, "Oxidation resistance of novel multilayer coatings for gas turbine components," Surf. Eng., vol. 30, no. 9, pp. 624–635, 2014.

[13] N. E. Beliardouh, K. Bouzid, C. Nouveau, B. Tlili, and M. J. Walock, "Tribological and electrochemical performances of Cr/CrN and Cr/CrN/CrAlN multilayer coatings deposited by RF magnetron sputtering," Trib. Inter., vol. 82, pp. 443–452, 2015.

[14] M. A. Al-Bukhaiti, K. A. Al-hatab, W. Tillmann, F. Hoffmann, and T. Sprute, "Tribological and mechanical properties of Ti/TiAlN/TiAlCN nanoscale multilayer PVD coatings deposited on AISI H11 hot work tool steel," Appl. Surf. Sci., vol. 318, pp. 180–190, 2014.

[15] Ö. Baran, F. Bidev, H. Çiçek, L. Kara, İ. Efeoğlu, and T. Küçükömeroğlu, "Investigation of the friction and wear properties of Ti/TiB2/MoS2 graded-composite coatings deposited by CFUBMS under air and vacuum conditions," Surf. Coat. Technol., vol. 260, pp. 310–315, 2014.

[16] S. Foppiano, S. J. Marshall, E. Saiz, A. P. Tomsia, and G. W. Marshall, "Functionally graded bioactive coatings: Reproducibility and stability of the coating under cell culture conditions," Acta Biomater., vol. 2, no. 2, pp. 133–142, 2006.

[17] T. S. N. S. Narayanan, I. Baskaran, K. Krishnaveni, and S. Parthiban, "Deposition of electroless Ni – P graded coatings and

evaluation of their corrosion resistance," Surf. Coat. Technol. vol. 200, pp. 3438–3445, 2006.

[18] W. X. Zhang, Z. H. Jiang, G. Y. Li, Q. Jiang, and J. S. Lian, "Electroless Ni-P / Ni-B duplex coatings for improving the hardness and the corrosion resistance of AZ91D magnesium alloy," Appl. Surf. Sci., vol. 254, pp. 4949–4955, 2008.

[19] T. S. N. S. Narayanan, K. Krishnaveni, and S. K. Seshadri, "Electroless Ni-P/Ni-B duplex coatings: Preparation and evaluation of microhardness, wear and corrosion resistance," Mater. Chem. Phys., vol. 82, no. 3, pp. 771–779, 2003.

[20] G. K. Williamson and W. H. Hall, "X-ray line broadening from filed aluminium and wolfram," Acta Metall., vol. 1, p. 22, 1953.

[21] D. T. Gawne and U. Ma, "Engineering properties of chromium plating and electroless and electroplated nickel," surf. eng., vol. 4, pp. 239–249, 1988.

[22] A. Leyland and a. Matthews, "On the significance of the H/E ratio in wear control: A nanocomposite coating approach to optimised tribological behaviour," Wear, vol. 246, no. 1–2, pp. 1–11, 2000.

[23] A. Matthews and A. Leyland, "Materials Related Aspects of Nanostructured Tribological Coatings," in 51st. Annual Technical Conferebce, 2008, pp. 40–45.

[24] L. Wang, Y. Gao, Q. Xue, H. Liu, and T. Xu, "A novel electrodeposited Ni – P gradient deposit for replacement of conventional hard chromium," Surf. Coat. Technol., vol. 200, pp. 3719–3726, 2006.